phys. stat. sol. (b) **229**, No. 3, 1111–1120 (2002)

Editor's Choice

Charge-Density-Wave Domain Originated Altshuler-Aronov-Spivak Effect in 1T-TaS_2 Single Crystal

T. Isa (a), M. Sasaki[1]) (b), G. R. Wu (a), Y. Isobe (a), W. X. Gao (c), and H. Ozaki (d)

(a) Graduate School of Advanced Sciences of Matter, Horishima University, Higashi-Hiroshima 739-8526, Japan

(b) Department of Physics, Faculty of Science, Yamagata University, Kojirakawa, Yamagata 990-8560 Japan

(c) Iwatani International Corporation, Moriyama, Siga 524-0041, Japan

(d) Department of Electronics, Electronics and Computer Engineering, Waseda University, Ohkubo 3-4-1, Shinjuku-ku, Tokyo 169-8555, Japan

(Received by M. S. Brandt July 13, 2001; accepted September 17, 2001)

Subject classification: 64.70.Rh; 71.45.Lr; 72.20.Pa; S8.11

We have performed photo-induced "transient thermoelectric effect (TTE)" experiments for charge-density-wave (CDW) material 1T-TaS_2 single crystals in hexagonal and triclinic nearly commensurate phases up to 5 T. The TTE voltages decay with the characteristic relaxation times τ_1, τ_2, and τ_3. τ_1 and τ_2 in the hexagonal phase oscillate with magnetic field B, while those in the triclinic phase are independent of B. The oscillatory phenomenon is interpreted by the Altshuler-Aronov-Spivak effect around the hexagonal arrays of commensurate CDW domains.

1. Introduction

It has been now well known that various *mesoscopic systems*, whose geometric size is comparable to the phase coherence length, show quantum interference (QI) phenomena, such as Aharonov-Bohm (AB) and Altshuler-Aronov-Spivak (AAS) effects. In both cases, the magnetoresistance oscillates with a constant periodicity ΔB under an applied magnetic field B, in sharp contrast to conventional Shubnikov-de Haas oscillations. The AB effect is due to the interference between separated wave packets of diffusing electrons where the periodicity is given by $\Delta B = (h/e)/S$ (S: cross sectional area of the system) [1, 2]. On the other hand, the AAS effect is due the phase interference between clockwisely and anti-clockwisely diffusing electrons; in this case the periodicity is written as $\Delta B = (h/e)/(2S)$ [3–5].

Recently we have found a similar behavior for the *bulk* charge-density-wave (CDW) material γ-Mo_4O_{11} with not mesoscopic but macroscopic scale, where the characteristic relaxation times τ_1 and τ_2 in the decay curves of the photoinduced "transient thermoelectric effect (TTE)" vary with a constant periodicity under a magnetic field [6]. This result has been attributed to the formation of any *microscopic domains* formed around the CDW pinning centers, but the detailed mechanism unexplained, since there is no clear evidence for such domain structures. In order to study such QI effects in a bulk

[1]) Corresponding author; e-mail: sasaki@sci.kj.yamagata-u.ac.jp

 0370-1972/02/22903-1111 $ 17.50+.50/0

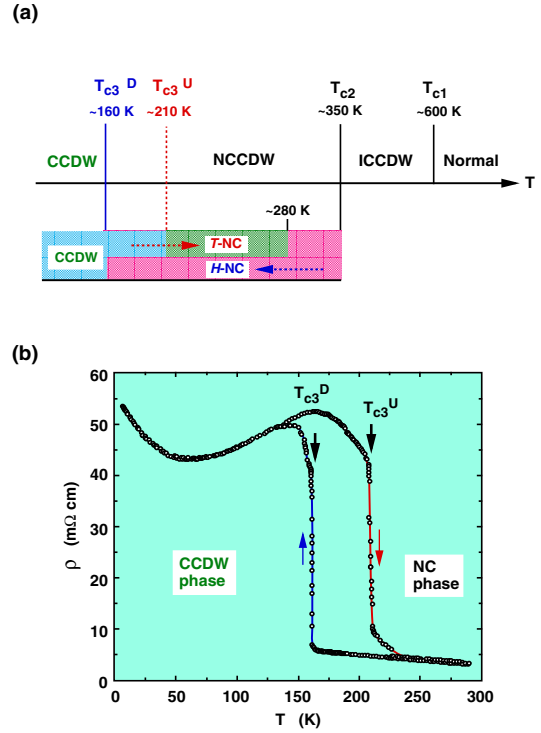

Fig. 1. a) Phase diagram of 1T-TaS_2 near T_{c3}. The horizontal arrows indicate cooling or heating processes. b) Typical temperature dependence of resistivity ϱ

CDW material system, we have selected the layered material 1T-TaS_2 that has clear domain structures.

As shown schematically in Fig. 1a, this material exhibits successively various phase transitions [7]. The system changes from normal to incommensurate CDW (denoted by ICCDW) at T_{c1} ($\approx$600 K), nearly commensurate (NC) CDW at T_{c2} ($\approx$352 K), and commensurate CDW (CCDW) at T_{c3}^D ($\approx$160 K) for a cooling process or at T_{c3}^U ($\approx$210 K) for a heating process (see Fig. 1b). Scanning tunneling microscopy has revealed that in the NC phase there exists a *hexagonal* array of CCDW domains (referred to as H-NC phase) surrounded by the ICCDW sea (see Fig. 6a) [8, 9]. In addition, the formation of *triclinic* CDW domains (T-NC) of elongated shape is also reported in the NC phase [10]. The hexagonal H-NC domains appear only when the temperature is lowered from the transition temperature T_{c2}, while the triclinic T-NC domains become stable when the temperature is raised from T_{c3}^U, and upon further heating above 280 K, the hexagonal H-NC phase appears again. Such CDW domains may play an important role in the transport properties of conduction carriers in a magnetic field.

In the present work, we have carried out TTE experiments for 1T-TaS_2 single crystals in the NC phase at 200–300 K. We have found AAS-like oscillations in the relaxation times of the TTE decay curves under a magnetic field. Based on these experimental results and a CDW domain model, we shall discuss its possible QI effect for bulk CDW material.

2. Experimental

1T-TaS_2 single crystals were grown by a chemical vapor transport method, in the same way as described by DiSalvo et al. [11]. A standard four-probe method was used to measure the dc and TTE voltages of the samples. The pulsed laser induced TTE measurements were made at the laser energy of 1.17 eV with a fixed laser intensity of about 10 mJ; experimental details have been reported elsewhere [12, 13]. The magnetic field B was applied perpendicular to the conducting layers (**B** $\perp$ **aa** plane) using a supercon-

ducting magnet. To realize the H-NC phase, the sample was first cooled down below T_{c3}^{D}, and then heated above T_{c3}^{U} up to ≈300 K, followed by cooling down again to 240 K, as noted above. The intensity of TTE signals in the H-NC phase was generally weak compared to those in the CCDW phase, and so a multiple averaging of 200–500 times was made to reduce the noises involved.

3. Experimental Results

Figure 2 shows the typical TTE signals at 240 K (H-NC phase) under magnetic field B up to 5 T. In zero magnetic field, the photoinduced TTE voltage V increases rapidly within a very short time interval of 0.1 μs, decays gradually until ≈2 μs, and then increases to approach zero. With increasing magnetic field B, its minimum is enhanced up to 2 T but above which it is suppressed. These TTE decay profiles can be expressed in the multiple exponential form [6, 12, 13],

$$V = V_0 + \Sigma\, a_i \exp\left(-t/\tau_i\right), \tag{1}$$

where V_0 is a constant value at $t \to \infty$, τ_i a relaxation time for the i-th relaxation process, and a_i the corresponding relaxation amplitude. According to earlier works [6, 12, 13], $a_i > 0$ corresponds to electrons, while $a_i < 0$ to holes. We have observed three relaxation processes with the characteristic relaxation times τ_1–τ_3 and corresponding amplitudes a_1–a_3 (a_1, $a_2 > 0$; $a_3 < 0$). The faster two processes with τ_1 and τ_2 are due to conduction electrons, while slow one with τ_3 is due to holes, as will be discussed later. Similar but no magnetic field dependent TTE signals were observed in the T-NC phase, though not shown here.

Figure 3 shows the temperature dependence of the relaxation times τ_1–τ_3, plotted in semi-logarithmic scales. Here, the experimental results obtained in the T-NC phase during the heating process are shown by squares, and those at 240 K and $B = 0$ in the H-NC phase are shown by circles. The solid and open symbols for the relaxation processes corresponds to $a_i > 0$ and $a_i < 0$, respectively. They are almost temperature independent. Both τ_1 and τ_2 in the H-NC phase are in agreement with those in the T-NC phase within experimental error, though τ_3 in the H-NC phase is slightly shorter compared with that in the T-NC phase. This suggests that the conduction electrons corresponding to τ_1 and τ_2 are essentially the same in both H- and T-NC phases. Since the magnitude of the slow relaxation process with τ_3 is very small, however, we could not say whether the holes related to τ_3 are the same in both phases.

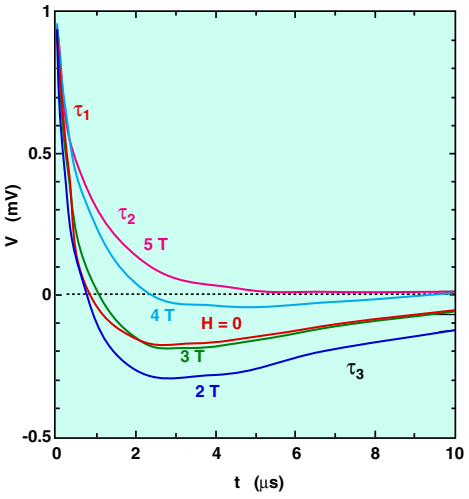

Fig. 2. TTE signals observed at 240 K under magnetic fields up to 5 T in the H-NC phase

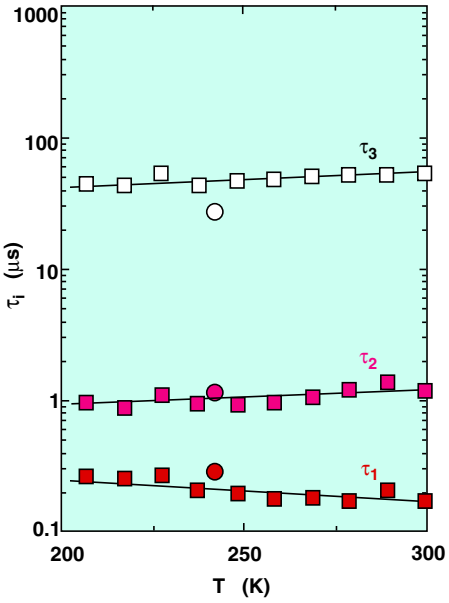

Fig. 3

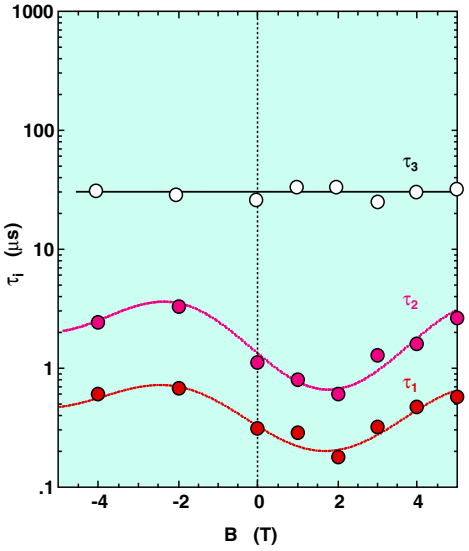

Fig. 4

Fig. 3. Temperature dependence of the relaxation times τ_1–τ_3

Fig. 4. Magnetic field dependence of the relaxation times τ_1–τ_3

Furthermore, we have performed TTE experiments at 240 K under magnetic fields B up to 5 T. Figure 4 shows the magnetic field dependence of the relaxation times τ_1–τ_3 in the H-NC phase. Both τ_1 and τ_2 show an asymmetric magnetic field dependence, while τ_3 is field-independent. However, τ_1–τ_3 in the T-NC phase are found to be field-independent, though not shown here. It should be emphasized that the oscillatory phenomena in the relaxation times τ_1 and τ_2 are observable only in the H-NC phase, where the H-NC domains exist. The periodicity of these oscillations is nearly $\Delta B = 8$–9 T. Usually, transport quantities as magnetoresistance do not show any field dependence in the high temperature range, say 240 K, and thus the anomalous field-dependent τ_1 and τ_2 cannot be interpreted by the conventional transport theory.

4. Discussion

4.1 Origin of TTE signals

According to our earlier work [12], the TTE decay processes consist of stage 1 (recombination process of the photogenerated electron–hole pairs), stage 2 (thermal diffusion of conduction carriers), and stage 3 (diffusion of phonons). Since stage 1 is observable typically in semiconductors and stage 3 is usually in the ms time region, stage 2 is responsible for the observed TTE decay processes in the present system as metal. Taking into account the signs of these processes, the processes related to τ_1 and τ_2 are due to thermal diffusion of photogenerated electrons along the concentration or temperature gradient produced by the pulsed laser irradiation, while the one concerned with τ_3 is due to holes.

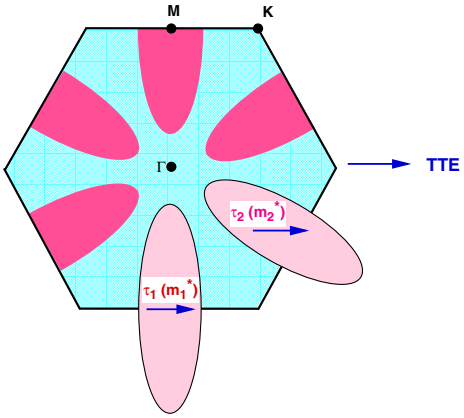

Fig. 5. Schematic picture of the Fermi surfaces in the original Brillouin zones. The arrows indicate the relationship between the direction of the TTE experiments and the relaxation times observed

Next we shall discuss the Fermi surfaces of 1T-TaS_2 in the NC phase, as depicted schematically in Fig. 5. In the normal phase, quasi-two-dimensional (Q2D) electron Fermi surfaces (lightly shaded areas) lie around the six equivalent ΓM lines (see Fig. 5) that have favorable shape for successive CDW nesting [7, 14–16]. Here, we illustrated rather simplified ellipsoidal Fermi surfaces: the whole shapes are depicted by thin solid ellipsoids in the extended Brillouin zones: this is similar to the case for bismuth [17]. If we assume that the direction of the TTE experiments is parallel to one of the principal axes of the ellipsoidal Fermi surfaces, we may observe two types of conduction electrons. In Fig. 5 we took the TTE direction along the MK direction and thus two electron pockets along the MK direction and four ones along the ΓK direction. Taking into account the band curvature, the former should have light effective mass, while the latter has heavy mass. We have another choice of the TTE direction along ΓK direction, which is essentially similar to the above: thus we are not concerned with this direction for the following discussion. On the other hand, the relaxation time τ for stage 2 is inversely proportional to the carrier mobility μ ($\tau \propto 1/\mu \propto m^*$; m^* effective mass). Thus, we can attribute τ_1 to the relaxation processes and τ_2 can be attributed to the thermal diffusion of electrons with m_1^* and m_2^* ($m_1^* < m_2^*$) along the MK and ΓK directions, respectively, as shown in Fig. 5. However, we cannot attribute the slow process with τ_3 to any conduction holes because of lack of detailed information on the real Fermi surfaces. Due to this reason and magnetic field-independent τ_3, we shall further discuss only τ_1 and τ_2.

4.2 Quantum interference model

The QI effect called AB or AAS effect is an interesting quantum transport phenomenon under magnetic field. Its characteristic field dependence is quite different from the conventional quantum transport such as Shubnikov-de Haas (SdH) oscillations, from the following viewpoints. (1) The QI effect oscillates in linear magnetic field B but the SdH appears in reciprocal magnetic field $1/B$. (2) The latter is not observed in weak magnetic field but the former is visible even in zero magnetic fields. (3) Usually the QI effect is observable in *mesoscopic systems* and at low temperature whose geometric size or sample length L_S is comparable to the phase coherence length ξ. The above characteristics (1) and (2) for the QI effect are also observable in the present oscillations of the relaxation times τ_1 and τ_2. In the previous work, we have observed similar phenomena in the quasi-two-dimensional material γ-Mo_4O_{11} in the CDW phase [6]. Only from the viewpoint (3), however, these systems with typically $L_S \approx 2$–3 mm are apparently

quite different from the *mesoscopic systems*. According to the TTE theory [6], on the other hand, the length scale occurring in the TTE voltage V is defined by the diffusion length L_i which is the mean distance of bipolar states formed by photo-induced carrier diffusion. The i-th relaxation time τ_i is expressed using the corresponding diffusion length L_i [12],

$$\tau_i = L_i^2/(2D_i) = eL_i^2/(2k_B T\mu_i)\,, \tag{2}$$

where D_i is the diffusion coefficient and μ_i the carrier mobility. Usually L_i ranges between 1 and 100 μm [18] and the roughly evaluated value of L_i for the present system was in the order of 1 μm just below T_{c3}^{D} (which will be reported elsewhere): $L_i \ll L_s$. It is expected that the magnitude of the diffusion length in the NC phase changes less strongly. This suggests the possibility that the QI may occur in the present system.

Among the theoretical studies on the QI in mesoscopic systems, we shall focus on the AAS effect in antidot lattices [19–21]. Nakanishi and Ando have demonstrated that in antidot arrays the AAS effect is predominant rather than the AB effect and is strongly influenced by the symmetry of arranged arrays. This gives us important key aspects to the origin of the present oscillatory phenomena. (i) the most definite difference between the AB and AAS effects can be seen in the magnitude of the magnetoconductance averaged over systems with many mesoscopic subsystems [22, 23]. The phase of the AB effect is *incoherent* in each subsystem and then cancels out after averaging over the whole system, giving rise to its diminishing. On the contrary, the AAS effect with *coherent* phases remains even in large systems involving small mesoscopic size units. Due to this reason, if the QI effect may occur in the present system only the AAS effect should be observed because the system consists of many H-NC or T-NC domains. (ii) The stronger backscattering occurs in hexagonal lattices rather than in square lattices; which is reflected in a larger AAS effect. This theoretical result gives us an important insight into the present experimental facts that the oscillatory phenomena in the relaxation times were observed not in the T-NC but in the H-NC phases. (iii) A *"fluctuation effect"* in antidot sizes enhances the AAS effect. This is an important effect because in real system the size of minimal regions exhibiting the AAS effect may fluctuate, as will be discussed later.

In the previous work, we have reported oscillatory phenomena in the relaxation times τ_1 and τ_2 for γ-Mo_4O_{11} single crystals and have proposed a possible model [6]. According to this model, we present a tentative model (model 1) as shown in Fig. 6a where only a few CCDW hexagonal domains existing in the ICCDW sea are illustrated. In this model, the conduction electrons move relatively freely in the ICCDW sea but they localize weakly in the CCDW domains. When an electron circulates within the CCDW domain, its phase changes by the magnetic flux ϕ penetrating through the closed hexagonal domain. In the present system, however, conduction electrons passing through the CCDW domains should be scattered strongly by the domain walls rather than by the CCDW domains because of destructron of translational symmetry of the phase at the domain walls. Therefore, this model may be ruled out from possible mechanisms. Considering the AAS effect in antidot lattices described above [19], thus, we proposed newly a possible model (model 2) for the transport of electrons in the H-NC phase, as shown in Fig. 6b. In this model, the electrons drift nearly freely inside the domains but are scattered strongly at the rigid domain walls, which play a similar role as in the antidots. It is expected that the dominant scattering process for model 2

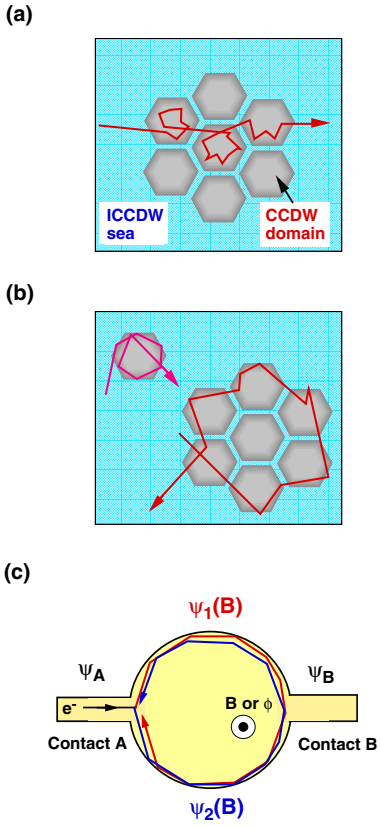

Fig. 6. Tentative models of the AAS mechanism. a) Model 1: the conduction electrons are localized in the CCDW domains. b) Model 2: the electrons are scattered by the rigid CCDW domain walls. c) Basic mechanism of the AAS process occurring in the model unit

should be backward scattering; though that for model 1 is predominantly forward scattering. In this case the electron scattering may depend strongly on the symmetry of the domain structures because the conduction carriers may be scattered easily backward by the hexagonal arrays of the CCDW domains rather than the elongated triclinic ones, as already shown theoretically [19]. For model 2, it is possible to consider several orbits or trajectories: for example orbits 1, 3, and 7 circulating one, three, and seven domains, respectively, in Fig. 6b the orbits 1 and 7 are depicted schematically. Hereafter "o1", "o3", and "o7" denote the orbits 1, 3, and 7, respectively.

Now let us discuss the AAS effect based on model 2, in which the number of averagings should diminish the AB effect. The period of aligned CCDW domains in the present system is about 9 nm at 240 K and the boundary between the domains is narrow ($\approx$0.2 nm) [8, 10]; from which the radius of the CCDW domains R_0 is evaluated to be $\approx$4.4 nm. Using this value, we have evaluated roughly the period of the AAS oscillations, ΔB_j [$= (h/e)/(2S_j) = (h/e)/(4\pi R_j^2)$; R_j radius of the orbit j], to be 32, 11, and 4.6 T for the orbits $j =$ o1, o3, and o7, respectively. Among them, the value of ΔB_{o3} for "o3" is nearly equal to the experimental value of $\Delta B \approx 9$ T. Since ΔB_{o1} for "o1" is too large, the AAS effect of electrons circulating "o1" is unlike in the present system. Here, we simply assume that the inelastic scattering length of diffusing electrons L_ϕ is much larger than the diameter of the orbits R_j and the scattering at the boundary is mostly elastic. In case of TTE experiments, the system size L can be regarded as the diffusion length L_i and the evaluated value of L_i for the present system was in the order of 1 μm, as described above. Under the consition $L_s \gg L_i > L_\phi > R_j$ we will consider the AAS effect for the electrons related to the relaxation times τ_1 and τ_2, while we do not discuss the relaxation time τ_4 for holes ($i = 1$ and 2; $j =$ o3 and o7).

4.3 Calculation of relaxation times

As can be seen from the trajectory of electron circulating "o7" in Fig. 6b, the electron drifts pass through diffusive CCDW domain walls and nearly ballistic CCDW regions. The

QI occurs only in the former regions but its theoretical approach is too hard to perform because of complicated trajectories. For simplicity, then, we introduced a simple model unit consisting of one diffusive region (where the orbit j exists) connected by contacts A and B (which corresponds to the ballistic CCDW regions) (see Fig. 6c). Here the electron with wave function Ψ_A at the contact A splits into a clockwise wave packet $\Psi_1(B)$ and an anti-clockwise one $\Psi_2(B)$, and then they interfere again at the contact A (not B) to form $\Psi_1(B) + \Psi_2(B) = \Psi_A \exp[2\pi i(\phi_j/2\phi_0)] = \Psi_A \exp[2\pi i(BS_j/2\phi_0)]$ [ϕ magnetic flux penetrating though the j-th closed trajectory; ϕ_0 flux quanta]. On the other hand, the Landauer formula for a finite size system is applied to this system [24] and then the transmittance $T_{AB}(B)_j$ of the electron between the contacts A and B is given by

$$T_{AB}(B)_j = T_{AB}(0)_j \exp[2\pi i(BS_j/2\phi_0)]. \tag{3}$$

To extend this aspect to the whole system, we further simplified the model 2 as follows. (i) We assume linear channels for conduction electrons, whose number is N_{ch} per unit cross sectional area, and each channel contains model units of number N_s. (ii) We consider electrons of number N_t passing through the unit model per second. (iii) Based on Onsager's theorem, the N_s times spatial and N_t times temporal averaging of the AAS effect occurring in each channel can be regarded as $N_s \times N_t$ times ensemble average of one electron in some channel. (iv) We neglect the contact resistance that may be much less than that of the diffusive domain. Therefore, the total conductance $G(B)_j$ is defined by

$$G(B)_j = N_{ch}/(N_s N_t)\,(e^2/h)\,\langle T(B)_j\rangle, \tag{4}$$

where $T(B)_j \equiv T_{AB}(B)_j$. Thus, the conductivity σ_1 related to the relaxation time τ_1 is expressed as

$$\sigma_1 = ne\mu_1 = \Sigma G(B)_j/L_1 = \Sigma N_{ch}/(N_s N_t L_1)\,(e^2/h)\,\langle T(B)_j\rangle, \tag{5}$$

where μ_1 is the mobility of electrons concerned with the relaxation time τ_1. This equation indicates that the microscopic magnetotransport is governed by the microscopic AAS effect. From Eqs. (2), (3), and (5), we obtain an important relationship between $\tau_1(B)$ under magnetic field B and $\langle T(B)_j\rangle$,

$$\tau_1(B) = nhN_s N_t L_1^3/[2N_{ch}k_B T\Sigma\,\langle T(0)_j \exp[2\pi i(BS_j/2\phi_0)]\rangle]. \tag{6}$$

In case of small AAS oscillations, the averaged transmittance in this equation is approximately written by

$$\langle T(0)_j \exp[2\pi i(BS_j/2\phi_0)]\rangle = \langle T(0)_j\rangle + \alpha_j \cos(B/\Delta B_j + \theta_j), \tag{7}$$

where α_j and θ_j are the amplitude and initial phase of the j-th AAS component, respectively. Therefore, the relaxation time $\tau_1(B)$ expressed by Eq. (6) is rewritten by

$$\tau_1(B) \sim \tau_1(0) - \Sigma\,\Delta\tau_j \sin(B/\Delta B_j + \theta_j) \tag{8}$$

with

$$\tau_1(0) = nCL_1^3/[k_B T\Sigma\,\langle T(0)_j\rangle], \quad \text{and} \quad \Delta\tau_j = nCL_1^3/[k_B T\alpha_j],$$

where $\Delta\tau_1$ is the amplitude of the AAS oscillation in the field-dependent τ_1 and $C(= hN_s N_t/2N_{ch})$ the parameter. Similarly, we obtain the expression for the relaxation

time $\tau_2(B)$ as: $\tau_2(B) \sim \tau_2(0) - \Sigma\,\Delta\tau_j \sin(B/\Delta B_j + \theta_j)$. Using the parameters related to the relaxation times $\tau_1 = 2.0\,\mu s$ and $\tau_2 = 0.45\,\mu s$, $\Delta\tau_1 = 1.4\,\mu s$, and $\Delta\tau_2 = 0.25\,\mu s$ and those concerned with the AAS orbits $\Delta B_{o3} = 11$ T, $\Delta B_{o7} = 4.6$ T, and $\theta_{o3} = \theta_{o7} = -60°$, we calculated $\tau_1(B)$ and $\tau_2(B)$ and the results are shown by solid lines in Fig. 4. These are in good agreement with the experimental results. This fact reveals that the present quantum oscillations in the relaxation times τ_1 and τ_2 are due to the AAS effect of electrons occurring in the CCDW domains. Finally we note the initial phases θ_1 and θ_2 whose observed values are non-zero (or π) ($\theta_1 = \theta_2 = -60°$). Such trends have been observed for γ-Mo_4O_{11} [6]. This may be due to non-linear transport.

5. Conclusion

We have performed TTE measurements for 1T-TaS_2 single crystals in both H- and T-NC phases and at 240 K under magnetic field up to 5 T. The TTE voltages decay with characteristic relaxation times τ_1 and τ_2 due to electron diffusions and τ_3 due to holes. Among them, τ_1 and τ_2 in the H-NC phase oscillate with magnetic field B, while those in the T-NC phase are independent of B. This phenomenon can be interpreted by the AAS effect. We have calculated their relaxation times based on the theoretical equations derived; where the oscillation of τ_1 and τ_2 are due to the AAS effect of electrons occurring the H-NC domains.

Acknowledgements We would like to express our thanks to Emeritus Prof. Masasi Inoue for his suggestion and Professor Michiko Miura for her encouragement through this work. We thank the Cryogenic Center, Hiroshima University for supplying liquid helium.

References

[1] Y. Aharonov and D. Bohm, Phys. Rev. **115**, 485 (1959).
[2] R. A. Webb, S. Washburn, A. D. Benoit, C. P. Umbach, and R. B. Laibowitz, Phys. Rev. Lett. **54**, 2696 (1985).
[3] B. L. Altshuler, A. G. Aronov, and B. Z. Spivak, Pisma Zh. Eskp. Teor. Fiz. **33**, 101 (1981) [Sov. Phys. – JETP Lett. **33**, 94 (1981)].
[4] D. Y. Sharvin and Y. V. Sharvin, Pisma Zh. Eskp. Teor. Fiz. **34**, 285 (1981) [Sov. Phys. – JETP Lett. **34**, 272 (1981)].
[5] C. P. Umbach, C. V. Haesindock, R. B. Laibowitz, S. Washburn, and R. A. Webb, Phys. Rev. Lett. **56**, 386 (1986).
[6] W. X. Gao, M. Sasaki, H. Negishi, K. Takase, and M. Inoue, J. Low Temp. Phys. **102**, 487 (1996).
[7] J. A. Willson, F. J. DiSalvo, and S. Mahajan, Adv. Phys. **24**, 117 (1975).
[8] X. L. Wu and C. M. Lieber, Phys. Rev. Lett. **64**, 1150 (1990).
[9] R. V. Coleman, W. W. McNairy, and C. G. Slough, Phys. Rev. B **45**, 1428 (1992).
[10] R. E. Thomson, B. Burk, A. Zettl, and J. Clarke, Phys. Rev. B **49**, 16899 (1994).
[11] F. J. DiSalvo, J. A. Wilson, B. G. Bagley, and J. V. Waszczak, Phys. Rev. B **12**, 2220 (1975).
[12] M. Sasaki, H. Negishi, and M. Inoue, J. Appl. Phys. **59**, 796 (1986).
[13] M. Sasaki, G. X. Tai, S. Tamura, and M. Inoue, Phys. Rev. B **46**, 1138 (1992).
[14] P. Blaha, K. Schwarz, P. Sorantin, and S. B. Trickey, Comput. Phys. Commun. **59**, 399 (1990).
[15] Th. Pillo, J. Hayoz, H. Beerger, R. Fasel, L. Schlapbach, and P. Aebi, Phys. Rev. B **62**, 4277 (2000).
[16] R. Claessen, B. Burandt, H. Carstensen, and M. Skibowski, Phys. Rev. B **41**, 8270 (1990).
[17] M. Sasaki, G. X. Tai, M. Koyano, H. Negishi, H. Bidadi, and M. Inoue, Physica B **194–196**, 1199 (1994).

[18] M. Sasaki, M. Koyano, and M. Inoue, J. Appl. Phys. **61**, 2267 (1987).
[19] T. Nakanishi and T. Ando, Phys. Rev. B **54**, 8021 (1996).
[20] S. Ishizaki, F. Nihey, K. Nakamura, J. Sone, and T. Ando, Jpn. J. Appl. Phys. **34**, 4317 (1995).
[21] S. Ishizaki, F. Nihey, K. Nakamura, J. Sone, and T. Ando, Phys. Rev. B **51**, 9881 (1995).
[22] C.-K. Sun, B. Golubovic, J. G. Fujimoto, H. K. Choi, C. A. Wang, and C. J. Stanton, Phys. Rev. B **50**, 8539 (1994).
[23] F. Nihey, S. W. Hwang, and K. Nakamura, Phys. Rev. B **51**, 4649 (1995).
[24] J. Singh, Physics of Semiconductors and Their Heterostructures, McGraw-Hill, New York 1993.

Minoru Sasaki
1978: PhD of Science; 1985: Associate Professor (Hiroshima University); 2001: Professor (Yamagata University)
Field: semiconductor physics, low temperature physics, and transport phenomena
Current affiliations: (i) development of the transient thermoelectric effect (TTE) and the transient Nernst effect; (ii) dynamic study of transport phenomena in various conductors using the TTE method, (iii) quantum Hall effect in bulk materials, (iv) simulation of sliding motion of charge-density waves, and (v) dynamic study of conduction carriers interacting with magnetic spins using the TTE method under magnetic field.